spectra are consistent with the local structure about each Mo atom, with two pyrazole rings trans to the CO's and one pyrazole ring trans to S (Se), but they provide no evidence concerning the existence of rotamers. However, the proton NMR spectra of **2** and its tungsten analogue, investigated by Hubbard and Lichtenberger,[8] do clearly show hindered rotation of each $(HB(Me_2pz)_3)(CO)_2M$ fragment about the M–S bonds.

Several complexes with linear M–X–M (X = S, Se) units are now known for group 6 metals in different oxidation states. The chemistry of these compounds has not yet been extensively explored. For molybdenum both $[Mo\text{–}S\text{–}Mo]^{2+}$ and $[Mo\text{–}S\text{–}Mo]^{6+}$ complexes are known. The existence of two stable classes of complexes differeing by four electrons suggests that a wealth of redox chemistry should exist for these systems.

Mo–S coordination is important in heterogeneous catalysts[19] and in biological systems.[20] Linear M–S–M units with short M–S bonds have now been demonstrated in both Co and Mo compounds. The possibility of a linear Co–S–Mo unit in CoMoS hydrodesulfurization catalysts should be considered. Finally, we note the unusually short Mo–S distances in **1** and **2** raise the interesting question as to whether such linear Mo–S–Mo structural features can be present in the enzyme xanthine oxidase, for which EXAFS spectroscopy has indicated[21] an Mo–S distance of ~2.15 Å. Current chemical and physical evidence strongly favors a mononuclear molybdenum site. However, the Mo···Mo distance of 4.4 Å for the Mo–S–Mo centers in **1** and **2** would probably not be detected by EXAFS spectroscopy.

**Acknowledgment.** Support of this research by the National Institutes of Environmental Health Sciences (Grant ES 00966) to J.H.E. and the National Science Foundation (Grant CHE 8310862) to S.K. is gratefully acknowledged. J.H.E. thanks the University of Arizona Computer Center for an allocation of computer time, K. Barnhart for technical assistance, and Dr. M. Minelli for the $^{95}$Mo NMR spectra.

**Registry No.** $1\cdot C_6H_5CH_3$, 95156-31-3; **2**, 90641-19-3; $3\cdot 2THF$, 95156-33-5; $(HB(pz)_3)Mo(CO)_3H$, 95156-34-6; S, 7704-34-9; $[Et_4N][(HB(Me_2pz)_3)Mo(CO)_3]$, 22357-70-6; Se, 7782-49-2.

**Supplementary Material Available:** Tables of anisotropic thermal parameters, calculated hydrogen positions, and structure factors for **1**, **2**, and **3** (39 pages). Ordering information is given on any current masthead page.

---

Contribution from the Departments of Chemistry, University of Hong Kong, Hong Kong,
and Chinese University of Hong Kong, Shatin, New Territories, Hong Kong

# Cis Ruthenium Complexes of 1,4,8,11-Tetraazacyclotetradecane (cyclam): Crystal and Molecular Structure of *cis*-$[Ru(cyclam)Cl_2]Cl$

CHI-MING CHE,*[1a] SI-SAN KWONG,[1a] CHUNG-KWONG POON,*[1a] TING-FONG LAI,[1a]
and THOMAS C. W. MAK[1b]

*Received July 11, 1984*

The crystal and molecular structure of *cis*-$[Ru(cyclam)Cl_2]Cl$ (cyclam = $C_{10}H_{24}N_4$) prepared by the $Ru(ox)_3^{3-}$ (ox = $C_2O_4^{2-}$) method has been determined: monoclinic, space group $P2_1/c$, $a = 7.579$ (1) Å, $b = 14.414$ (4) Å, $c = 14.718$ (3) Å, $\beta = 102.33$ (1)°, $V = 1570.8$ (5) Å$^3$, $Z = 4$. The average Ru–Cl distance, 2.371 (1) Å in the present complex, is substantially longer than that found in the corresponding trans isomer [2.342 (1) Å], reflecting the greater $\sigma$-trans effect of the secondary amine N atom over the chloride ligand. Reaction of *cis*-$[Ru(cyclam)Cl_2]Cl$ with N heterocyclic amines and Zn(Hg) yielded *cis*-$[Ru(cyclam)L_2]^{2+}$ ($L_2$ = $(py)_2$, bpy, phen), the metal-to-ligand charge-transfer transitions of which have been found to be blue shifted from those of the corresponding *cis*-$[Ru(NH_3)_4L_2]^{2+}$ species.

## Introduction

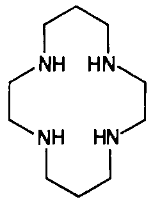

cyclam

In 1980, Isied reported the isolation of *cis*-$[Ru(cyclam)Cl_2]Cl$[2] (cyclam = 1,4,8,11-tetraazacyclotetradecane) as a by product during the synthesis of the *trans* isomer by the method of Chan et al. by reacting $K_2[RuCl_5H_2O]$ with cyclam in methanol.[3] Following this work, we reported a reaction scheme for the preparation of cis ruthenium(III) macrocyclic tetraamine species, utilizing $K_3[Ru(ox)_3]$ (ox = $C_2O_4^{2-}$) as the starting material.[4] The IR spectrum of our *cis*-$[Ru(cyclam)Cl_2]Cl$ in the most discriminating 800–900-cm$^{-1}$ region is very similar to those of all other well-characterized *cis*-$[M(cyclam)Cl_2]^+$ species[4] [M = Co(III), Cr(III), Fe(III)]; however, Isied's species showed a different IR spectrum. As for the electronic spectrum, the observed $\epsilon$ values (200–500 dm$^3$ mol$^{-1}$ cm$^{-1}$) for the bands above 300 nm of Isied's species are too low to be consistent with what would have been expected for ligand-to-metal charge-transfer transitions. Apparently, our cis-$[Ru(cyclam)Cl_2]Cl$ and Isied's species could not be the same compound. In order to resolve this structural ambiguity we have recently carried out an X-ray crystal structural determination of our *cis*-$[Ru(cyclam)Cl_2]Cl$ prepared by the $Ru(ox)_3^{3-}$ method. The results clearly indicate a cis configuration. This paper describes the X-ray structural analysis of our *cis*-$[Ru(cyclam)Cl_2]Cl$ and the synthetic chemistry of this species with some N heterocyclic amine ligands.

## Experimental Section

$K_2[RuCl_5H_2O]$ (Johnson and Matthey) was used as supplied. cyclam (cyclam = 1,4,8,11-tetraazacyclotetradecane) was twice recrystallized before use. All other reagents used were of analytical grade, and doubly distilled water was used throughout the experiments. $K_3[Ru(ox)_3]$ and *cis*-$[Ru(cyclam)Cl_2]Cl$ were prepared by literature methods,[4] with some minor modifications.

**$K_3[Ru(ox)_3]$.** $K_2[RuCl_5H_2O]$ (2 g, 5.3 mmol) and oxalic acid dihydrate (2.3 g, 18 mmol) in $H_2O$ were refluxed for $2^1/_2$ h during which the solution turned brown. Solid potassium carbonate was added continually in small amounts until the the solution reached ca pH 7 and the evolution of $CO_2$ subsided. After heating at just boiling for another 20 min, the resulting olive green solution was ready for use in the preparation of *cis*-$[Ru(cyclam)Cl_2]Cl$, without the need of isolating the pure $K_3[Ru(ox)_3]$.

***cis*-$[Ru(cyclam)Cl_2]Cl$.** A partially neutralized aqueous solution of cyclam was first prepared by adding HCl (2 M) to an aqueous solution of cyclam (1 g in 25 cm$^3$ $H_2O$) until the pH of the solution was ca. 6.5. This solution was slowly added to a freshly prepared solution of $[Ru(ox)_3]^{3-}$, and the pH was adjusted to ca. 7 with either potassium carbo-

---

(1) (a) University of Hong Kong. (b) Chinese University of Hong Kong.

(2) Isied, S. S. *Inorg. Chem.* **1980**, *19*, 911–914.

(3) Chan, P. K.; Isabirye, D. A.; Poon, C. K. *Inorg. Chem.* **1975**, *14*, 2579–80.

(4) Poon, C. K.; Che, C. M. *J. Chem. Soc., Dalton Trans.* **1981**, 1336–1341.

(5) Brown, G. M.; Sutin, N. *J. Am. Chem. Soc.* **1979**, *101*, 883–892.

0020-1669/85/1324-1359$01.50/0

nate or HCl (2 M) as appropriate. The resulting solution was refluxed for 3 h during which time the color of the solution gradually turned brown. Concentrated hydrochloric acid (10 cm$^3$) was added to the brown solution that was then further refluxed for 30 min. Some dark gray precipitates formed at this stage were filtered off. The solution was then rotary evaporated until some yellow precipitates were formed. After the mixture was cooled to room temperature, more bright yellow precipitates of *cis*-[Ru(cyclam)Cl$_2$]Cl appeared and they were collected by filtration. The filtrate was allowed to cool in an ice bath for complete precipitation of some white solid that was then filtered off. Concentrated HCl (10 cm$^3$) was added to the filtrate, and the solution was rotary evaporated to about 20 cm$^3$. On cooling, another crop of the complex was obtained. The crude *cis*-[Ru(cyclam)Cl$_2$]Cl might be contaminated with a red substance that was removed by dissolving the crude complex in HCl (1 M; 20 cm$^3$) at 40 °C. On addition of concentrated HCl (5 cm$^3$) to the filtered solution, bright yellow crystals of *cis*-[Ru(cyclam)Cl$_2$]Cl slowly appeared and they were collected, washed with ice-cold water and an ethanol–diethyl ether mixture (1:10), and dried in vacuo at room temperature (yield 40%). The complex was unstable in neutral aqueous solution.

***cis*-[Ru(cyclam)L$_2$](PF$_6$)$_2$ [L$_2$ = bpy (2,2′-Bipyridine) or phen (1,10-Phenanthroline)].** These two complexes were prepared by the same method with similar yields (40–60%), as described in detail for *cis*-[Ru(cyclam)(bpy)](PF$_2$)$_6$.

*cis*-[Ru(cyclam)Cl$_2$]Cl (0.06 g, 0.15 mmol) was stirred with several pieces of amalgamated zinc in H$_2$O (15 cm$^3$) under an argon atmosphere for 15 min. 2,2-Bipyridine (bpy) (0.033 g, 0.2 mmol) was then added to the solution. After 2 h, a dark red solution was obtained. The solution was filtered, and excess bpy was removed by extraction with CHCl$_3$ (3 × 10 cm$^3$). Dropwise addition of a saturated solution of NaPF$_6$ to the resulting solution gave a dark red crystalline solid that was filtered off and washed with ice-cold water and an ethanol–diethyl ether mixture (1:10). The crude product was recrystallized by dissolving it in acetone followed by the addition of diethyl ether; yield ~0.06 g (55%). Anal. Calcd for *cis*-[Ru(cyclam)(bpy)](PF$_6$)$_2$: C, 32.14; H, 4.32; N, 11.24. Found: C, 32.11; H, 4.47; N, 11.16. *cis*-[Ru(cyclam)(phen)][PF$_6$]$_2$ was similarly prepared as a dark red solid. Anal. Calcd for *cis*-[Ru(cyclam)(phen)](PF$_6$)$_2$: C, 34.25; H, 4.18; N, 10.89. Found: C, 34.39; H, 3.82; N, 10.70.

***cis*-[Ru(cyclam)(py)$_2$][PF$_6$]$_2$ (py = Pyridine).** *cis*-[Ru(cyclam)Cl$_2$]Cl (0.06 g) and amalgamated zinc (2 g) were stirred in degassed H$_2$O (10 cm$^3$) for 10 min. A degassed solution of pyridine (py) (1 cm$^3$) in ethanol (10 cm$^3$) was added, and the resulting solutions was kept at 40 °C under an argon atmosphere for 2 h. This was then filtered to remove the unreacted zinc, and the filtered solution was rotary evaporated to dryness. The crude yellow solid obtained was then stirred with an aqueous solution of NaPF$_6$ (1 g in 10 cm$^3$ H$_2$O). A bright yellow precipitate was formed, and this was filtered off and washed with ice-cold water and an ethanol–diethyl ether mixture (1:10). The crude *cis*-[Ru(cyclam)(py)$_2$](PF$_6$)$_2$ could be recrystallized by dissolving it in acetone followed by the addition of diethyl ether; yield ~45%. Anal. Calcd for *cis*-[Ru(cyclam)(py)$_2$](PF$_6$)$_2$: C, 32.60; H, 4.56; N, 10.90. Found: C, 32.05; H, 4.57; N, 11.21.

**Physical Measurements.** Elemental analyses of the newly prepared complexes were performed by Australian Microanalytical Service Unit. Infrared and electronic absorption spectra were recorded on a Perkin-Elmer 577 and Beckmann Acta CIII spectrophotometer, respectively. $^1$H NMR spectra were obtained in either CD$_3$CN or acetone-*d* on a JEOL FX 90Q FT spectrometer. Cyclic voltammograms were obtained with Princeton Applied Research (PAR) instruments: Model 175 (Universal Programmer) and Model 173 (potentiostat-galvanostat). A homemade graphite electrode was used as the working electrode. All reaction solutions were dearerated before the CV scans.

## X-ray Structure Determination

*cis*-[Ru(cyclam)Cl$_2$]Cl crystallizes from HCl (2 M) as brown prisms elongated along the *a* axis. A crystal block of approximate dimension 0.30 × 0.28 × 0.20 mm was centered on a Nicolet R3m four-circle diffractometer (graphite-monochromatized Mo K$\alpha$ radiation, $\lambda$ = 0.71069 Å), and determinations of the crystal class, orientation matrix, and accurate unit cell parameters were performed according to established procedures.[6]

**Crystal Data**: C$_{10}$H$_{24}$N$_4$Cl$_3$Ru, $M_r$ = 407.76, monoclinic, space group $P2_1/c$, $a$ = 7.579 (1) Å, $b$ = 14.414 (4) Å, $c$ = 14.718 (3) Å, $\beta$ = 102.33 (1)°, $V$ = 1570.8 (5) Å$^3$, $D_{\text{mead}}$(flotation in CCl$_4$–BrCH$_2$CH$_2$Br) = 1.725 g cm$^{-3}$, $Z$ = 4, $D_{\text{calcd}}$ = 1.724 g cm$^{-3}$, $F$(000) = 828, $\mu$(Mo K$\alpha$) = 14.85 cm$^{-1}$.

Table I. Atomic Coordinates (×10$^5$ for Ru and Cl; ×10$^4$ for N and C) and Equivalent Isotropic Thermal Parameters[a] (Å$^2$ × 10$^4$ for Ru and Cl; Å$^2$ × 10$^3$ for N and C)

| atom | $x$ | $y$ | $z$ | $U_{\text{eq}}$[b] |
|---|---|---|---|---|
| Ru | 19987 (4) | 24041 (2) | 9987 (2) | 279 (1) |
| Cl(1) | 648 (15) | 14109 (9) | 16212 (8) | 479 (4) |
| Cl(2) | 11143 (20) | 36647 (9) | 18382 (9) | 563 (5) |
| Cl(3) | 56448 (14) | 29016 (9) | 41909 (8) | 446 (4) |
| N(1) | 4327 (4) | 2167 (3) | 2057 (2) | 34 (1) |
| N(2) | 2667 (4) | 1272 (2) | 235 (2) | 32 (1) |
| N(3) | −21 (5) | 2607 (2) | −217 (3) | 34 (1) |
| N(4) | 3741 (5) | 3324 (2) | 509 (3) | 36 (1) |
| C(1) | 4779 (6) | 1179 (4) | 2314 (3) | 45 (2) |
| C(2) | 5043 (6) | 578 (3) | 1503 (3) | 44 (2) |
| C(3) | 3329 (6) | 420 (3) | 763 (3) | 40 (1) |
| C(4) | 1043 (6) | 1069 (3) | −501 (3) | 44 (2) |
| C(5) | 321 (6) | 1959 (3) | −950 (3) | 45 (2) |
| C(6) | −296 (6) | 3568 (4) | −589 (4) | 49 (2) |
| C(7) | 1387 (8) | 4012 (4) | −778 (4) | 57 (2) |
| C(8) | 2898 (7) | 4183 (3) | 35 (4) | 56 (2) |
| C(9) | 5232 (7) | 3546 (4) | 1309 (4) | 51 (2) |
| C(10) | 5883 (6) | 2655 (3) | 1794 (4) | 47 (2) |

[a] Esd's given in parentheses. [b] Calculated as one-third of the trace of the orthogonalized U matrix.

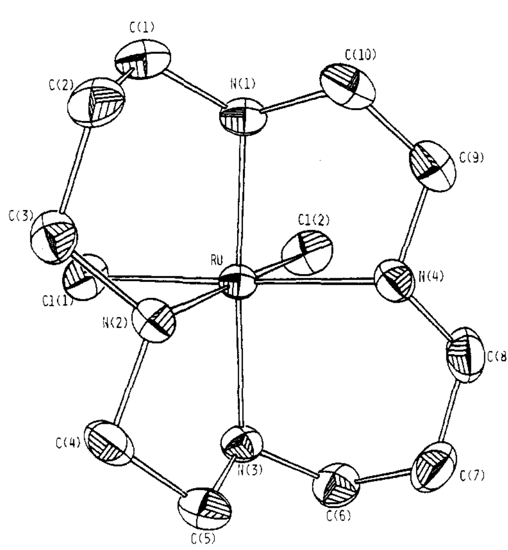

**Figure 1.** ORTEP plot of the cation *cis*-[Ru(cyclam)Cl$_2$]$^+$.

Intensities ($h$, $k$, ±$l$; 3441 unique data) were measured at 22 °C by using the $\omega$–$2\theta$ variable-scan (2.02–8.37° min$^{-1}$) technique in the bisecting mode up to $2\theta_{\max}$ = 54°. Azimuthal scans of selected strong reflections over a range of $2\theta$ values were used to define a pseudoellipsoid for the application of absorption correction ($\mu r$ = 0.20, tranmission factors 0.599–0.636).[7,8] The structure was solved by the heavy-atom method, and all non-hydrogen atoms were varied anisotropically. The methylene and amino H atoms were generated geometrically. They were allowed to ride on their respective parent C and N atoms with fixed C–H and N–H bond distances (both 0.96 Å). Isotropic temperature factors were also assigned. Convergence for 3081 ($n$) observed data ($|F_o| > 3\sigma|F_o|$) and 163 variables ($p$) was reached at $R \equiv \sum\Delta/\sum|F_o| = 0.032$ and $R_w \equiv [\sum w\Delta^2/\sum w|F_o|^2]^{1/2} = 0.058$, where $\Delta \equiv ||F_o| - |F_c||$ and $w = [\sigma^2(|F_o|) + 0.0005|F_o|^2]^{-1}$. The goodness-of-fit index $S \equiv [\sum w\Delta^2/(n - p)]^{1/2}$ has the value 1.774. The final difference Fourier map showed residual extrema in the range +0.44 to −0.63 e Å$^{-3}$, with the three highest peaks lying in the neighborhood of the Ru atom.

All computations were performed on a Data General Nova 3/12 minicomputer with the SHELXTL system of crystallographic programs.[9] Analytical expressions of neutral-atom scattering factors incorporating the real and imaginary components of anomalous dispersion were em-

---

(6) Sparks, R. A. "Crystallographic Computing Techniques"; Ahmed, F. R., Ed.; Munksgaard: Cophenhagen, 1976; p 452.

(7) Kopfmann, G.; Huber, R. *Acta Crystallogr., Sect. A: Cryst. Phys., Diffr., Theor. Gen. Crystallogr.* **1968**, *A24*, 348–351.

(8) North, A. C. T.; Phillips, D. C.; Mathews, F. S. *Acta Crystallogr., Sect. A: Cryst. Phys., Diffr., Theor. Gen. Crystallogr.* **1968**, *A24*, 351–359.

(9) Sheldrick, G. M. "Computational Crystallography"; Sayre, D., Ed.; Oxford University Press: New York, 1982; p 506.

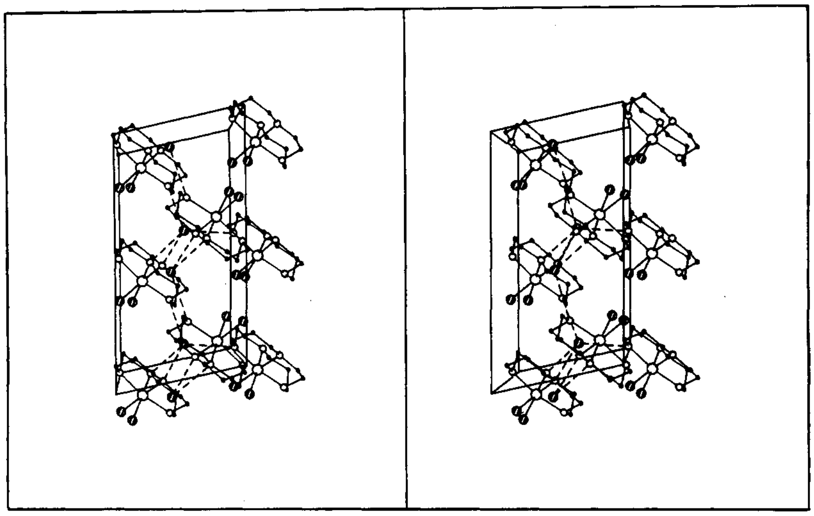

**Figure 2.** Stereoview of the crystal structure of *cis*-[Ru(cyclam)$Cl_2$]Cl. The unit cell origin lies at the upper left corner, with *a* pointing from left to right, *b* toward the reader, and *c* downward. Broken lines represent N–H···Cl interactions.

Table II. Some Major Bond Distances (Å)

| | | | |
|---|---|---|---|
| Ru–Cl(1) | 2.369 (1) | Ru–Cl(2) | 2.373 (1) |
| Ru–N(1) | 2.117 (3) | Ru–N(2) | 2.104 (3) |
| Ru–N(3) | 2.112 (3) | Ru–N(4) | 2.105 (4) |
| N(1)–C(1) | 1.494 (6) | N(1)–C(10) | 1.494 (6) |
| N(2)–C(3) | 1.482 (5) | N(2)–C(4) | 1.485 (5) |
| N(3)–C(5) | 1.492 (6) | N(3)–C(6) | 1.486 (6) |
| N(4)–C(8) | 1.495 (6) | N(4)–C(9) | 1.483 (6) |
| C(1)–C(2) | 1.523 (7) | C(2)–C(3) | 1.524 (6) |
| C(4)–C(5) | 1.493 (7) | C(6)–C(7) | 1.506 (8) |
| C(7)–C(8) | 1.489 (7) | C(9)–C(10) | 1.501 (7) |

Table III. Some Major Bond Angles (deg)

| | | | |
|---|---|---|---|
| Cl(1)–Ru–Cl(2) | 89.7 (1) | Cl(1)–Ru–N(1) | 96.1 (1) |
| Cl(2)–Ru–N(1) | 91.4 (1) | Cl(1)–Ru–N(2) | 88.7 (1) |
| Cl(2)–Ru–N(2) | 177.6 (1) | N(1)–Ru–N(2) | 90.6 (1) |
| Cl(1)–Ru–N(3) | 90.9 (1) | Cl(2)–Ru–N(3) | 95.8 (1) |
| N(1)–Ru–N(3) | 170.1 (2) | N(2)–Ru–N(3) | 82.5 (1) |
| Cl(1)–Ru–N(4) | 177.1 (1) | Cl(2)–Ru–N(4) | 87.9 (1) |
| N(1)–Ru–N(4) | 82.4 (1) | N(2)–Ru–N(4) | 93.8 (1) |
| N(3)–Ru–N(4) | 91.0 (1) | Ru–N(1)–C(1) | 116.8 (3) |
| Ru–N(1)–C(10) | 108.3 (3) | C(1)–N(1)–C(10) | 111.3 (4) |
| Ru–N(2)–C(3) | 117.1 (3) | Ru–N(2)–C(4) | 106.6 (3) |
| C(3)–N(2)–C(4) | 110.7 (3) | Ru–N(3)–C(5) | 108.6 (2) |
| Ru–N(3)–C(6) | 117.4 (3) | C(5)–N(3)–C(6) | 110.4 (4) |
| Ru–N(4)–C(8) | 116.4 (3) | Ru–N(4)–C(9) | 106.9 (3) |
| C(8)–N(4)–C(9) | 111.7 (3) | N(1)–C(1)–C(2) | 113.9 (4) |
| C(1)–C(2)–C(3) | 114.2 (4) | N(2)–C(3)–C(2) | 113.1 (3) |
| N(2)–C(4)–C(5) | 108.8 (4) | N(3)–C(5)–C(4) | 108.8 (4) |
| N(3)–C(6)–C(7) | 114.0 (4) | C(6)–C(7)–C(8) | 117.2 (5) |
| N(4)–C(8)–C(7) | 114.6 (4) | N(4)–C(9)–C(10) | 108.1 (4) |
| N(1)–C(10)–C(9) | 109.1 (4) | | |

Table IV. Hydrogen Bonds[a] (Å) and Selected Torsion Angles (deg)

| Distances | | | |
|---|---|---|---|
| Cl(3)···N(1) | 3.263 | Cl(3)···H(1) | 2.477 |
| Cl(3)···N(2)$^{I}$ | 3.218 | Cl(3)···H(2)$^{I}$ | 2.275 |
| Cl(3)···N(3)$^{II}$ | 3.296 | Cl(3)···H(3)$^{II}$ | 2.535 |
| Cl(3)···N(4)$^{I}$ | 3.188 | Cl(3)···H(4) | 2.253 |

| Angles | |
|---|---|
| N(1)–C(1)–C(2)–C(3) | −67.4 (5) |
| C(2)–C(3)–N(2)–C(4) | 177.6 (4) |
| N(2)–C(4)–C(5)–N(3) | −55.3 (5) |
| C(5)–N(3)–C(6)–C(7) | −69.9 (5) |
| C(6)–C(7)–C(8)–N(4) | 65.5 (6) |
| C(8)–N(4)–C(9)–C(10) | 174.9 (4) |
| C(9)–C(10)–N(1)–C(1) | 165.3 (4) |
| C(1)–C(2)–C(3)–N(2) | 68.4 (5) |
| C(3)–N(2)–C(4)–C(5) | 174.5 (4) |
| C(4)–C(5)–N(3)–C(6) | 165.8 (4) |
| N(3)–C(6)–C(7)–C(8) | −64.4 (6) |
| C(7)–C(8)–N(4)–C(9) | 180.0 (5) |
| N(4)–C(9)–C(10)–N(1) | −55.6 (5) |
| C(10)–N(1)–C(1)–C(2) | −67.5 (5) |

[a] Key: (I) $x$, $\frac{1}{2} - y$, $\frac{1}{2} + z$; (II) $1 - x$, $\frac{1}{2} - y$, $\frac{1}{2} + z$.

ployed.[10] Final positional and thermal parameters of non-hydrogen atoms are tabulated in Table I. Tables of hydrogen atomic coordinates, anisotropic thermal parameters, and structure factors are available as supplementary material.

## Results and Discussion

**Description of the Structure of *cis*-[Ru(cyclam)$Cl_2$]Cl.** Figure 1 is an ORTEP plot of the cation and shows the atom-numbering scheme. Major bond distances and bond angles are given in Tables II and III, respectively. Figure 2 is a stereoview of the molecular packing in the unit cell of *cis*-[Ru(cyclam)$Cl_2$]Cl. The chloride ligands are cis to each other as in the original assignment,[4] and the cation has approximately $C_2$ symmetry, with a pseudo-2-fold axis bisecting the Cl–Ru–Cl angle. The six-membered chelate rings have a chair conformation while the two five-membered rings are gauche (see torsion angles in Table IV). The unit cell consists of enantiomeric pairs of cations in the cis *RRRR* and cis *SSSS* configurations. The *R,S* designation is based on the sequence rule of Cahn, Ingold, and Prelog[13] and serves to indicate the helicity of the four nitrogen centres. It is quite possible that this is the most stable form for metal complexes containing a cyclam ligand in the cis configuration. An analogous structure has also been reported for *cis*-[Co(cyclam)(en)]$^{3+}$.[14]

Bond distances within the cation are not unusual. The average Ru–Cl distance, 2.371 (1) Å in the present complex, is substantially longer than that found in the corresponding *trans*-[Ru(cyclam)$Cl_2$]$^+$ species [2.342 (1) Å].[15] This probably reflects the greater σ-trans effect of the secondary amine N atom over the chloride ligand and also correlates well with the finding that *cis*-[Ru(cyclam)$Cl_2$]$^+$ is much more substitutionally labile than the corresponding trans species.[16] The average Ru–N distance of 2.110 (4) Å is comparable to that found in Ru(en)$_3^{3+}$ (2.11 Å)[17] or Ru(NH$_3$)$_6^{3+}$ (2.104 Å).[18] Bond distances and angles

---

[10] "International Table for X-Ray Crystallography"; Kynoch Press: Birmingham, England, 1974; Vol. 4, pp 99, 149.

[11] Broomhead, J. A.; Kane-Maquire, L. A. P. *J. Chem. Soc. A* **1967**, 546–553.

[12] Poon, C. K.; Che, C. M. *J. Chem. Soc., Dalton Trans.* **1981**, 1919–1923.

[13] Cahn, R. S.; Ingold, C. K.; Prelog, V. *Angew. Chem., Int. Ed. Engl.* **1966**, *5*, 385–415.

[14] Lai, T. F.; Poon, C. K. *Inorg. Chem.* **1976**, *15*, 1562–1566.

[15] Walker, D. D.; Taube, H. *Inorg. Chem.* **1981**, *20*, 2828–2834.

[16] Kwong, S. S.; unpublished results.

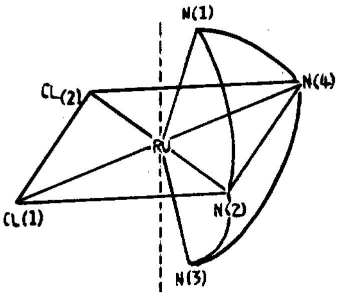

**Figure 3.** Illustration of distortion of ligand donor atoms from octahedral positions.

**Table V.** Electronic Spectral Data of Some Cis Ruthenium Tetraamine Complexes

| complex | solvent | $\lambda_{max}$, nm (log $\epsilon$) |
|---|---|---|
| *cis*-$[Ru(NH_3)_4Cl_2]Cl^a$ | HCl | 352 (3.21), 310 (3.14), 262 (2.80) |
| *cis*-$[Ru(en)_2Cl_2]Cl^b$ | HCl | 354 (3.24), 314 (3.15), 269 (2.95) |
| *cis*-$[Ru(cyclam)Cl_2]Cl^c$ | HCl | 380 (br, 3.03), 336 (br, 3.17), 276 (br, 2.98) |
| *cis*-$[Ru(NH_3)_4(py)_2]^{2+\,d}$ | $H_2O$ | 410 (3.90), 375 (3.81), 245 (3.86) |
| *cis*-$[Ru(en)_2(py)_2]^{2+\,e}$ | $H_2O$ | 398 (4.0), 370 (3.96), 243 (3.97) |
| *cis*-$[Ru(cyclam)(py)_2]^{2+}$ | $H_2O$ | 378 (4.1), 340 (sh, 3.70), 245 (3.99) |
| *cis*-$[Ru(NH_3)_4(bpy)]^{2+\,e}$ | $H_2O$ | 522 (3.24), 366 (3.76), 295 (4.51), 244 (4.0) |
| *cis*-$[Ru(en)_2(bpy)]^{2+\,e}$ | $H_2O$ | 513 (3.53), 362 (3.72), 293 (4.27), 243 (3.89) |
| *cis*-$[Ru(cyclam)(bpy)]^{2+}$ | $H_2O$ | 504 (3.66), 359 (3.81), 294 (4.12), 243 (4.00) |
| *cis*-$[Ru(NH_3)_4(phen)]^{2+\,e}$ | $H_2O$ | 471 (3.82), 265 (4.54) |
| *cis*-$[Ru(en)_2(phen)]^{2+\,e}$ | $H_2O$ | 500 (sh), 466 (3.88), 340 (sh, 3.37), 264 (4.55) |
| *cis*-$[Ru(cyclam)(phen)]^{2+}$ | $H_2O$ | 500 (sh, 3.8), 458 (3.86), 340 (sh, 3.36), 324 (sh, br, 3.39), 266 (4.55) |
| *trans*-$[Ru(NH_3)_4(py)_2]^{2+\,d}$ | $H_2O$ | 423 (4.22), 245 (3.93) |

[a] Reference 20. [b] Reference 11. [c] Reference 4. [d] Reference 19. [e] Kwong, S. S., unpublished results.

within the chelate rings correspond closely to those of *cis*-$[Co(cyclam)(en)]^{3+}$.[14] The Ru–N–C angles within the six-membered rings are close to 117°, suggesting the presence of appreciable strain. The N–Ru–N angles range from 82.4 to 96.1°, indicating that coordination around the central ruthenium is that of a distorted octahedron. The primary distortion appears to involve the two diagonally opposite nitrogens atoms being bent away from an axis normal to the Cl–Ru–Cl plane (Figure 3). As shown in the unit cell packing diagram (Figure 2), the crystal structure is consolidated by $N-H\cdots Cl^-$ interactions in the range 3.18–3.30 Å (Table IV), presumably hydrogens bonds, utilizing all available amino H atoms.

**General Chemistry and Spectroscpopic Properties.** $K_3[Ru(ox)_3]$ has been used successfully as a starting material for the synthesis of cis ruthenium(III) tetraamine complexes.[4,11] Reduction of *cis*-$[Ru(cyclam)Cl_2]Cl$ with amalgamated zinc yielded *cis*-$[Ru(cyclam)(H_2O)_2]^{2+}$, which on reaction with N heterocyclic amine L (L = py; $L_2$ = bpy, phen) gave *cis*-$[Ru(cyclam)L_2]^{2+}$. All the newly prepared complexes are stable in aprotic solvents and in the absence of air but gradually decompose in aerobic aqueous solution, especially at a high pH. In aqueous solution, *cis*-$[Ru(cyclam)Cl_2]^{2+}$ gradually changed its color to dark green. Similarly, aerobic aqeous solutions of *cis*-$[Ru(cyclam)(bpy)]^{2+}$ and *cis*-$[Ru(cyclam)(phen)]^{2+}$ changed from red to yellow within 24 h. $^1H$ NMR studies of the resulting solution in $D_2O$ indicated the presence of diimine protons ($\delta$ ~9–10). We attribute that this decomposition reaction was due to a ligand oxidative dehydrogenation reaction. Similar observations have also been reported for other ruthenium amine species.[12]

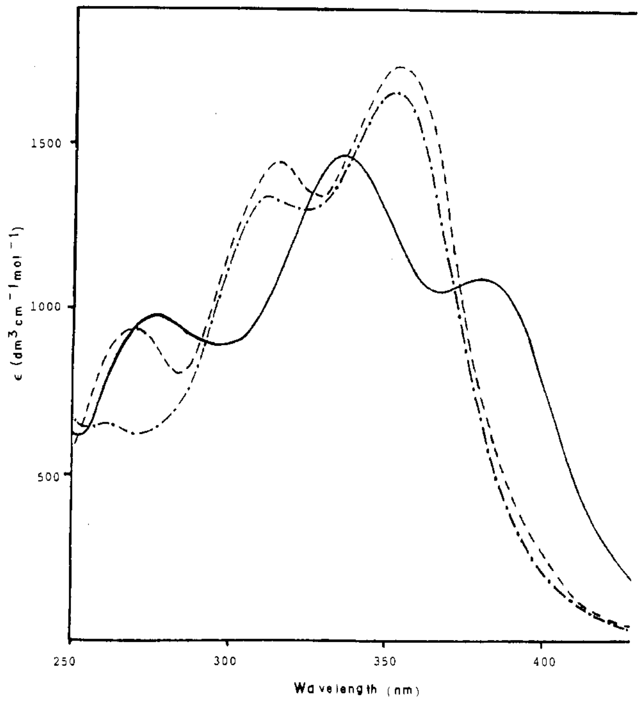

**Figure 4.** UV–Vis absorption spectra of *cis*-$[RuA_4Cl_2]^+$ [$A_4$ = $(NH_3)_4$, $(en)_2$, cyclam] in HCl (0.1 M): --- *cis*-$[Ru(en)_2Cl_2]^+$; —, *cis*-$[Ru(cyclam)Cl_2]^+$; -·-, *cis*-$[Ru(NH_3)_4Cl_2]^+$.

**Table VI.** Electrochemical Data for Some Ru(III)/Ru(II) Couples

| couple | $E_{1/2}$ (vs. NHE),[a] mV |
|---|---|
| *cis*-$[Ru(NH_3)_4(py)_2]^{3+/2+}$ | 0.505[b] |
| *cis*-$[Ru(NH_3)_4(bpy)]^{3+/2+}$ | 0.510[c] |
| *cis*-$[Ru(NH_3)_4(phen)]^{3+/2+}$ | 0.510[c] |
| *cis*-$[Ru(en)_2(bpy)]^{3+/2+}$ | 0.590[d] |
| *cis*-$[Ru(en)_2(phen)]^{3+/2+}$ | 0.550[e] |
| *cis*-$[Ru(cyclam)(py)_2]^{3+/2+}$ | 0.574 |
| *cis*-$[Ru(cyclam)(bpy)]^{3+/2+}$ | 0.650 |
| *cis*-$[Ru(cyclam)(phen)]^{3+/2+}$ | 0.630 |

[a] All potentials were measured in 0.1 M $CF_3SO_3H$ unless otherwise stated in references. [b] Matsubara, T.; Ford, P. C. *Inorg. Chem.* 1976, *15*, 1107–1110. [c] Brown, G. M.; Sutin, N. *J. Am. Chem. Soc.* 1979, *101*, 883–892. [d] Kwong, S. S., unpublished results. [e] Mahoney, D. F.; Beattie, J. K. *Inorg. Chem.* 1973, *12*, 2561–2565.

Table V is a collection of electronic absorption spectral data of some cis ruthenium(II)/ruthenium(III) tetraamine complexes. The UV–vis absorption spectra of *cis*-$[RuA_4Cl_2]^+$ [$A_4$ = $(NH_3)_4$, $(en)_2$, cyclam) are shown in Figure 4. With reference to the simplified molecular orbital model of Zwickel and Creutz,[19] two metal-to-ligand charge-transfer (MLCT) transitions $d^*_\pi \rightarrow \pi^*(py)$ are predicted for *cis*-$[RuA_4(py)_2]^{2+}$. Vanquickenborne and his co-workers,[20] using the treatment of Zwickel and Creutz, also predicted two allowed ligand-to-metal charge-transfer (LMCT) transitions $p_\pi(Cl) \rightarrow d^*_\pi$ of equal intensities for *cis*-$[RuA_4Cl_2]^+$ species. For *cis*-$[Ru(cyclam)Cl_2]^+$, three bands in the UV–vis region are observed. The two lowest energy bands are assigned as the $p_\pi(Cl) \rightarrow d^*_\pi$ transitions, whereas the 260–280-nm band, that is also present in trans-$[RuA_4Cl_2]^+$,[21] is probably due to the $p_\sigma(Cl) \rightarrow d^*_\pi$ transition. For *cis*-$[Ru(cyclam)(py)_2]^{2+}$, the 378- and 340-nm bands are assigned as the MLCT: $d^*_\pi \rightarrow \pi^*(py)$

---

(17) Peresie, H. J.; Stanko, J. A. *J. Chem. Soc. D* **1970**, 1674–1675.
(18) Stynes, H. C.; Ibers, J. A. *Inorg. Chem.* **1971**, *10*, 2304–2308.
(19) Zwickel, A. M.; Creutz, C. *Inorg. Chem.* **1971**, *10*, 2395–2399.
(20) Verdonck, E.; Vanquickenborne, L. G. *Inorg. Chem.* **1974**, *13*, 762–764.
(21) Poon, C. K.; Lau, T. C.; Che, C. M. *Inorg. Chem.* **1983**, *22*, 3893–3898.

Table VII. Infrared Spectra of *cis*-$[Ru(cyclam)L_2](PF_6)_2$ ($L_2$ = $(py)_2$, bpy, phen) in the 3500–300-, 1700–1400- and 800–600-$cm^{-1}$ Regions

| complexes | abs bands, $cm^{-1}$ | | |
|---|---|---|---|
| | NH stretch | $CH_2$, NH, C=C, or C=N vibrations | |
| *cis*-$[Ru(cyclam)(py)_2](PF_6)_2$ | 3292 (s), 3090 (w) | 1602 (w), 1490 (s), 1450 (s) | 765 (vs), 748 (s), 710 (vs), 630 (w), |
| *cis*-$[Ru(cyclam)(bpy)](PF_6)_2$ | 3272 (m), 3300 (s) | 1608 (w), 1425 (s) | 795 (m), 768 (vs), 744 (m), 738 (s), 660 (w), 652 (w), 630 (w) |
| *cis*-$[Ru(cyclam)(phen)](PF_6)_2$ | 3310 (s), 3290 (sh) | 1603 (m), 1430 (s), 1420 (m) | 795 (w), 785 (w), 750 (m), 732 (vs), 630 (w) |

[a] Abbreviations: s, strong; m, medium; w, weak; vs, very strong.

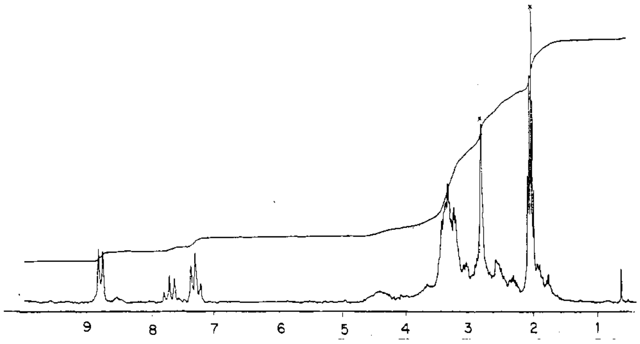

**Figure 5.** $^1H$ NMR spectrum of *cis*-$[Ru(cyclam)(py)_2]^{2+}$ in $CD_3CN$ with $Me_4Si$ as internal reference.

transitions. For the bpy and phen complexes, a detailed spectral assignment is not possible in the present study. However, it is still reasonable to assign the bands in the visible region as MLCT transitions on the basis of their intensities. Similarly, the strong bands in the 250–300-nm region are possibly internal ligand $\pi \rightarrow \pi^*$ transitions that are commonly observed for ruthenium complexes containing N heterocycles. It has been found that increasing chelation around the central ruthenium ion red shifts the LMCT bands but has the reverse effect on the MLCT transitions. Previously, we attributed the chelation effect on LMCT transitions of ruthenium(III) amine complexes as primarily due to the solvation effect.[21] It is quite likely that the increasing hydrophobic nature of the complexes with increasing chelation would make the $p_\pi$ electrons of $L_2$ in *cis*-$[Ru(A_4)L_2]^{2+}$ less solvated, hence leading to an overall increase in their relative energy levels. As the $d^*_\pi$ levels are not much affected by solvation, the MLCT bands will be blue shifted with increasing chelation around the central ion. Alternatively, one may assume that the MLCT transition will generate a polar excited state:

$$Ru^{II}L \xrightarrow{h\nu} Ru^{III}L^-$$

Since the extent of solvation decreases in the order $(NH_3)_4$ > $(en)_2$ > cyclam, the MLCT excited state of *cis*-$[Ru(NH_3)_4L_2]^{2+}$ is most stabilized and hence its transition energy will be the smallest. The $E_f°$ values of *cis*-$[RuA_4L_2]^{2+}$ (Table VI) have been found to increase from $(NH_3)_4$ to cyclam, and this is in agreement with the solvation effect.

The clear and well-resolved $^1H$ NMR spectra of the newly prepared *cis*-$[Ru(cyclam)L_2]^{2+}$ indicated the absence of any paramagnetic species. No detailed assignments have been made because of the complexity of the spectra. However, the absence of any peaks at ca. $\delta$ 9.0–10 in *cis*-$[Ru(cyclam)(py)_2]^{2+}$ (Figure 5) clearly indicates the absence of any imine protons that could have been resulted by ligand dehydrogenations.[12] Aliphatic protons could not be resolved well under the present experimental conditions. Nevertheless, the observed ratios of all aliphatic to aromatic protons are in good agreement with the assigned formula of the complexes.

The IR data of *cis*-$[Ru(cyclam)L_2]^{2+}$ and the related complexes are collected in Table VII. The IR spectra of the coordinated N heterocyclic ligands resemble closely to those of the corresponding free ligands, except with minor shifts in positions, splittings, and intensities. The observed splitting of the $\nu$(N–H) stretch at ca. 3300–3100 $cm^{-1}$ in *cis*-$[Ru(cyclam)L_2]^{2+}$ is also consistent with a cis configuration of these complexes. The absence of any intense bands at ca. 1600 $cm^{-1}$ in *cis*-$[Ru(cyclam)(py)_2]^{2+}$ clearly indicates the absence of any dehydrogenated impurities.

**Acknowledgment.** We thank the Committee on Research and Conference Grants of the University of Hong Kong for financial support.

**Registry No.** *cis*-$[Ru(cyclam)Cl_2]Cl$, 72300-89-1; $K_3[Ru(ox)_3]$, 29475-51-2; *cis*-$[Ru(cyclam)(bpy)](PF_6)_2$, 95346-42-2; *cis*-$[Ru(cyclam)(phen)](PF_6)_2$, 95346-44-4; *cis*-$[Ru(cyclam)(py)_2](PF_6)_2$, 95346-46-6; *cis*-$[Ru(en)_2(py)_2]^{2+}$, 95346-47-7; *cis*-$[Ru(NH_3)_4(bpy)]^{2+}$, 54194-87-5; *cis*-$[Ru(en)_2(bpy)]^{2+}$, 95346-48-8; *cis*-$[Ru(NH_3)_4(phen)]^{2+}$, 69799-59-3; *cis*-$[Ru(en)_2(phen)]^{2+}$, 95346-49-9; *cis*-$[Ru(cyclam)(py)_2]^{3+}$, 95346-50-2; *cis*-$[Ru(cyclam)(bpy)]^{3+}$, 95346-51-3; *cis*-$[Ru(cyclam)(phen)]^{3+}$, 95346-52-4.

**Supplementary Material Available:** Tables of hydrogen atom parameters (Table VIII), anisotropic temperature factors (Table IX), and observed and calculated structure factors (Table X) (20 pages). Ordering information is given on any current masthead page.